Characteristics of Indium-Tin-Oxide Nanoparticles Prepared by Controlled Chemical Coprecipitation Method

Hyun Woo Kim and Yeong Il Kim[*]

*Department of Chemistry, Pukyong National University, Busan 608-737, Korea. *E-mail: ykim@pknu.ac.kr*
Received May 21, 2008

Sn-doped In_2O_3, usually called indium-tin-oxide (ITO), has been widely utilized in optoelectronic devices as a form of thin film due to its high electrical conductivity and transparency to visible light.[1] Recent studies of ITO have been focused on shape and size controlled nanoparticles for the versatile device applications.[2] The crystal structure of ITO nanoparticles follows that of In_2O_3 that is known to have two types of crystal structures: bixbyite structure of cubic unit cell[3a] and corundum structure of rhombohedral or hexagonal unit cell.[3b] While most of pure In_2O_3 or ITO nanoparticles were fabricated as bixbyite type, not many reports of corundum type nanoparticles are known despite the corundum type ITO has some advantages such as higher specific gravity and more stable conductivity. This is just because of synthetic difficulty of the high temperature and high pressure condition.[4] Recently Qian *et al.* reported the hydrothermal method of synthesizing ITO or In_2O_3 nanoparticles and nanowire of corundum structure in a relatively mild conduction.[5] Gurlo *et al.* also synthesized corundum type In_2O_3 in ambient pressure condition using acetylacetone/methanol solvent condition.[6] Lee *et al.* reported uniformly size-controlled nanocubes of corundum In_2O_3 prepared by surfactant-assisted method.[7] All these recent studies revealed that corundum type In_2O_3 could be obtained through the dehydration of InOOH. Here, we report the preparation of corundum ITO nanoparticles by the simple temperature and pH controlled coprecipitation in aqueous solution.

Figure 1 shows X-ray diffraction patterns of ITO precursors that were prepared at different pHs and temperatures in aqueous solution. When the precursor was prepared at pH 12, it consisted of mainly cubic $In(OH)_3$ at 60 °C and some unknown phases were mixed with cubic $In(OH)_3$ at 0 and 30 °C. However, when the precursor was prepared at pH 8, it was almost amorphous at 0 and 30 °C and showed dominantly orthorhombic InOOH structure at 60 °C as shown in Figure 1(b). When these ITO precursors were annealed above 300 °C, the structural transformation occurred. As shown in Figure 2, the precursors that were prepared at pH 12 were transformed to bixbyite structure ITO regardless of precipitation temperature when they were annealed at 400 °C for 2 hours. Whereas, those prepared at pH 8 were changed to bixbyite or corundum type ITO at the same condition depending on the precipitation temperature: corundum for the precipitate at 60 °C, bixbyite for the precipitate at 0 and

30 °C. The XRD patterns of bixbyite ITO whose precursors were prepared at pH 8 are much sharper and well defined than those prepared at pH 12. The unit cell parameter *a* that was calculated from Nelson-Riley extrapolation for the precursor prepared at pH 8 and 0 °C is closest to the known bulk value (10.118 Å)[3a] as 10.112 Å. The values for the other precursors were a little smaller than this. The particle sizes calculated from Debye-Scherrer equation tells that the lower precipitation temperature was, the smaller the particle size was in the case of pH 12. On the contrary, what was prepared at lower precipitation temperature showed larger particle in the case of pH 8. The crystallization of the precursors prepared at pH 8 to bixbyite structure occurred
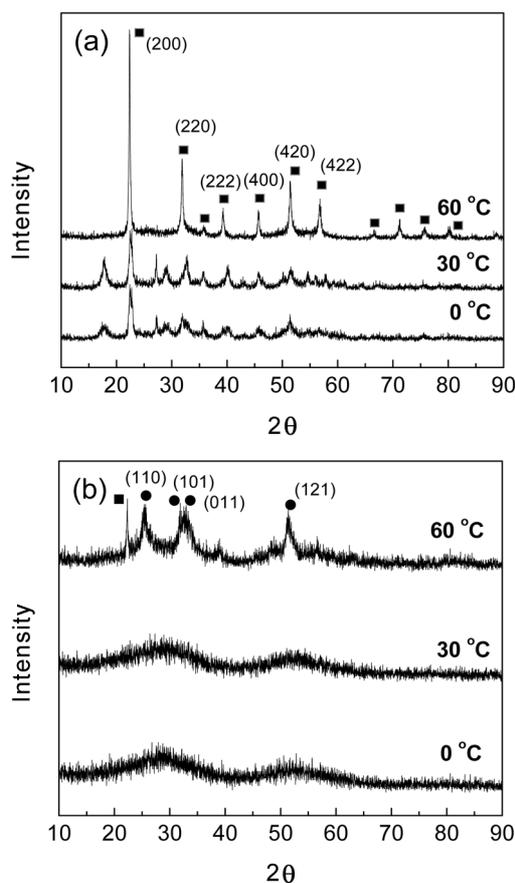

Figure 1. XRD patterns of ITO precursors that were precipitated at various temperatures and pH 12 (a) and 8 (b) without heat treatment. ■ and ● represent XRD peaks of $In(OH)_3$ and InOOH, respectively.
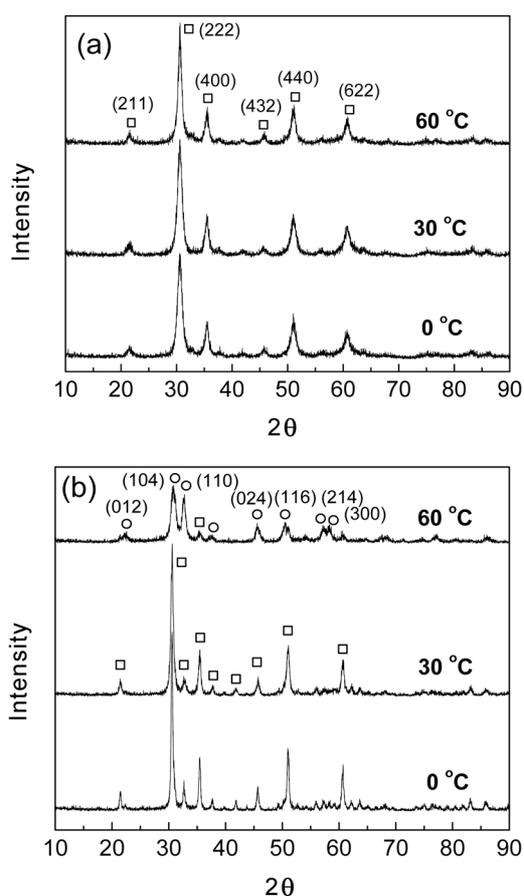
Figure 2. XRD patterns of ITO nanoparticles that were prepared by annealing of ITO precursors at 400 °C shown in Figure 1: (a) precipitated at pH 12 and (b) at pH 8. □ and ○ represent XRD peaks of cubic and rhombohedral In_2O_3, respectively.

Figure 3. TGA curves of ITO precursors that were prepared at various temperatures and pH 12 (a) and 8 (b).

from amorphous phase, while the precursors prepared at pH 12 were transformed mainly from cubic $In(OH)_3$ to cubic In_2O_3 although some mixed phases existed in them prepared at lower temperatures. The crystallization from amorphous phase may be easier than from another crystal phase because of lower activation energy. For this reason the XRD patterns of ITO prepared at pH 8 are much sharper than those prepared at pH 12. The unit cell parameters of the corundum structure ITO were calculated as 5.474 and 14.522 Å for *a* and *c*, respectively. The a value is a little smaller and the c value is a little larger than those of the known corundum In_2O_3 that were prepared at high pressure and temperature (65 kbar and 110 °C).[3b]

The thermogravimetric analysis (TGA) and differential scanning calorimetric (DSC) data show clearly the difference between the precursors prepared at pH 12 and 8. For all three precursors prepared at pH 12 the weight losses occurred similarly about 17% sharply until about 300 °C as shown in Figure 3(a). These losses are coincident to the theoretical weight loss (16.3%) when $In(OH)_3$ transforms to In_2O_3. DSC data show that the transformation temperatures shown as endothermic peaks in Figure 4(a) systematically increased as the precipitation temperature increased. For the precursors prepared at pH 8 the situation was more complex. The pre-
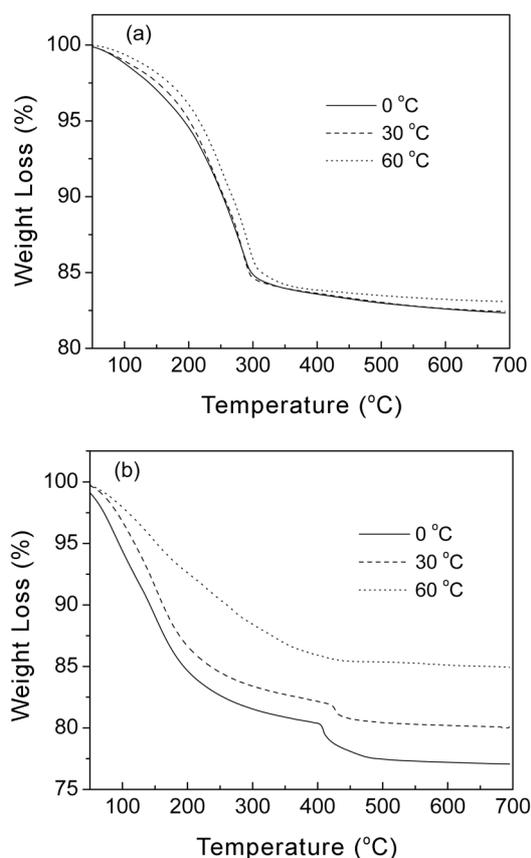
cursors prepared at 0 and 30 °C show two stages of weight losses and sharp exothermic transformations in Figure 3(b) and 4(b). The precursor prepared at lower temperature showed more weight loss. The precursors prepared at 0 and 30 °C may be in the form of metastable hydroxide hydrate. The larger weight loss than for the precursors at pH 12 and the exothermic transformation might be explained by the dehydration from this metastable form. On the other hand, the precursor prepared at 60 °C show one stage smooth weight loss and no sharp phase transition in the Figures. The theoretical weight loss for the transformation from InOOH to In_2O_3 is 6.1%. In this case the loss was about 13%. This discrepancy may come from the fact the precursor was hydrated in the form of $InOOH \cdot xH_2O$. And no sharp phase transition may be due to the low crystallinity as shown in its XRD data.

Figure 5 shows HR-TEM pictures and electron diffraction (ED) patterns of ITO nanoparticle samples that were prepared at pH 8 and 0 °C and 60 °C. The ED patterns show clearly the difference between the samples prepared at 0 °C and 60 °C, of which crystal structure correspond to bixbyite and corundum, respectively. The particle sizes are both about 10-20 nm and the particle morphologies in both cases are also similar from the pictures of field-emission scanning electron microscopic pictures (not shown here). The particles in both cases exhibits lattice fringes that indicate their single
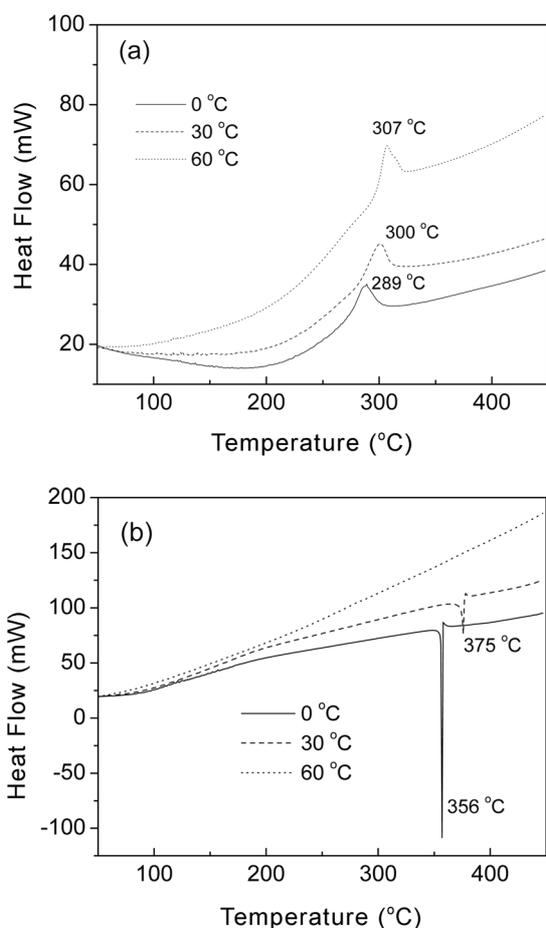
Notes

Bull. Korean Chem. Soc. **2008**, Vol. 29, No. 9   1829

Figure 4. DSC curves of ITO precursors that were prepared at various temperatures and pH 12 (a) and 8 (b) (up endothermic).
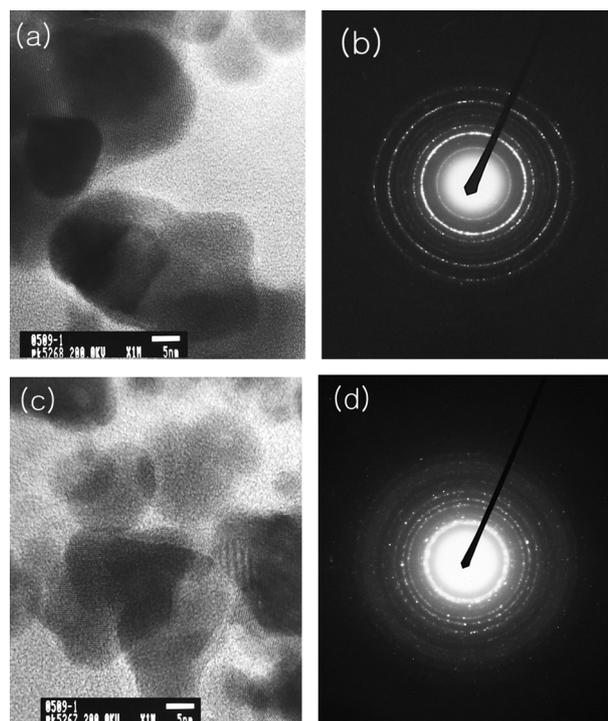

Figure 5. HR-TEM pictures and electron diffraction patterns of ITO nanoparticles that were prepared at pH 8 and 0 °C (a, b) and 60 °C (c, d).

crystal nature. The lattice plane distances approximately corresponds to the (222) and (104) planes for bixbyite and corundum structures, respectively.

In this study we have demonstrated that the crystal structure of ITO nanoparticles could be controlled by the precipitation condition of the precursors that were prepared by simple coprecipitation in aqueous solution. At pH 12 the precursors were crystallized as cubic $In(OH)_3$ structure regardless of precipitation temperatures herein studied and the subsequent annealing of the precursors above 300 °C gave only cubic bixbyite ITO. However, when the precursor was prepared at pH 8, it was amorphous or of orthorhombic InOOH structure depending on precipitation temperature. The only orthorhombic InOOH precursor that was prepared at 60 °C resulted in corundum structure of ITO, while the others gave the cubic bixbyite ITO structure. The result shows clear evidence that only rhombohedral InOOH can be transformed to the corundum structure, while cubic and amorphous $In(OH)_3$ give rise to bixbyite structure after dehydration.

Experimental

Synthesis of ITO nanoparticles. The mixture solution of

0.018 mol $In(NO_3)_3 \cdot 5H_2O$ (99.9%, Aldrich) and 0.002 mol $SnCl_4 \cdot 5H_2O$ (98%, Aldrich) in 50 mL of 0.4 M HCl was slowly introduced drop-by-drop into 300 mL of 1.5 M NaOH solution that was previously adjusted to appropriate pH with conc. HCl. During the addition of the mixed solution, the solution of 1.5 M NaOH was simultaneously added to keep an appropriate pH. The temperature of the reaction solution was maintained constant within ± 1 °C with a circulating thermostatic bath and water-jakected reaction vessel and the solution was vigorously stirred. The white precipitates appeared immediately with dropping of the mixed solution and the reaction solution was kept stirred for 1 hour after all mixture solution was added. The precipitates were centrifuged at 12,000 rpm for 10 minutes and washed with deionized water. The centrifugation and washing were repeated 5-8 times until the washed water was free from Cl^- and NO_3^- ions. The washed precipitates were dried under vacuum at an ambient temperature. The dried and aggregated precipitates were ground in agate mortar and calcined for 2 hours at various temperatures in air.

Apparatus. XRD patterns were obtained with Phillips X'Pert-MPD X-ray diffractometer with $CuK\alpha$ and 0.02°/sec scan rate. Thermal analysis data were measured with Perkin-Elmer Pyris 1 DSC and TGA 7 with 10 °C/min scan rate under N_2 atmosphere. FE-SEM and TEM pictures were taken with Hitachi H7500 and Jeol JEM-2010, respectively.

References

1. (a) Hartnagel, H. L.; Dawar, A. L.; Jain, A. K.; Jagdish, C. *Semiconducting Transparent Thin Films*; IOP Publishing: Bristol and Philadelphia, 1995. (b) Kim, Y.-I.; Yoon, J.-B.; Choy, J.-H.; Campet, G.; Camin, D.; Portier, J.; Salardenne, J. *Bull. Korean Chem. Soc.* **1998**, *19*, 107. (c) Lee, S. H.; Lee, J. H.; Kim, K. H.; Jun, J. H. *Bull. Korean Chem. Soc.* **1989**, *10*, 418.

2. (a) Kim, D. W.; Oh, S.-G.; Lee, J.-D. *Langmuir* **1999**, *15*, 1599. (b) Kim, K. Y.; Park, S. B. *Mater. Chem. Phys.* **2004**, *86*, 210. (c) Song, J. E.; Lee, D. K.; Kim, H. W.; Kim, Y. I.; Kang, Y. S. *Colloids Surf. A* **2005**, *257-258*, 539. (d) Wang, C.; Chen, D.; Jiao, X.; Chen, C. *J. Phys. Chem. C* **2007**, *111*, 13398.

3. (a) JCPDS No. 06-0416. (b) JCPDS No. 22-0336.

4. Prewitt, C. T.; Shannon, R. D.; Rogers, D. B.; Sleight, A. W. *Inorg. Chem.* **1969**, *8*, 1985.

5. (a) Yu, D.; Wang, D.; Lu, J.; Qian, Y. *Inorg. Chem. Comm.* **2002**, *5*, 475. (b) Yu, D.; Yu, S.-H.; Ahang, S.; Zuo, J.; Wang, D.; Qian, Y. *Adv. Funct. Mater.* **2003**, *13*, 497. (c) Yu, D.; Wang, D.; Qian, Y. *J. Solid State Chem.* **2004**, *177*, 1230.

6. Epifani, M.; Sicillano, P.; Gurlo, A.; Barsan, N.; Weimar, U. *J. Am. Chem. Soc.* **2004**, *126*, 4078.

7. Lee, C. H.; Kim, M.; Kim, T.; Kim, A.; Paek, J.; Lee, J. W.; Choi, S.-Y.; Kim, K.; Park, J.-B.; Lee, K. *J. Am. Chem. Soc.* **2006**, *128*, 9326.